The Discovery of Capsazepine, the First Competitive Antagonist of the Sensory Neuron Excitants Capsaicin and Resiniferatoxin

Christopher S. J. Walpole,* Stuart Bevan, Guenter Bovermann,† Johann J. Boelsterli,† Robin Breckenridge,† John W. Davies, Glyn A. Hughes, Iain James, Lukas Oberer,† Janet Winter, and Roger Wrigglesworth

Sandoz Institute for Medical Research, 5 Gower Place, London WC1E 6BN, U.K.

Received February 2, 1994•

Capsaicin and resiniferatoxin are natural products which act specifically on a subset of primary afferent sensory neurons to open a novel cation-selective ion channel in the plasma membrane. These sensory neurons are involved in nociception, and so, these agents are targets for the design of a novel class of analgesics. Although synthetic agonists at the capsaicin receptor have been described previously, competitive antagonists at this receptor would be interesting and novel pharmacological agents. Structure–activity relationships for capsaicin agonists have previously been rationalized, by ourselves and others, by dividing the capsaicin molecule into three regions—the A (aromatic ring)-, B (amide bond)-, and C (hydrophobic side chain)-regions. In this study, the effects on biological activity of conformational constraint of the A-region with respect to the B-region are discussed. Conformational constraint was achieved by the introduction of saturated ring systems of different sizes. The resulting compounds provided agonists of comparable potency to unconstrained analogues as well as a moderately potent antagonist, capsazepine. This compound is the first competitive antagonist of capsaicin and resiniferatoxin to be described and is active in various systems, *in vitro* and *in vivo*. It has recently attracted considerable interest as a tool for dissecting the mechanisms by which capsaicin analogues evoke their effects. NMR spectroscopy and X-ray crystallography experiments, as well as molecular modeling techniques, were used to study the conformational behavior of a representative constrained agonist and antagonist. The conformation of the saturated ring contraint in the two cases was found to differ markedly, dramatically affecting the relative disposition of the A-ring and B-region pharmacophores. In agonist structures, the A- and B-regions were virtually coplanar in contrast to those in the antagonist, in which they were approximately orthogonal. A rationale for agonist and antagonist activity at the capsaicin receptor is proposed, based on the consideration of these conformational differences.

Introduction

Capsaicin, the pungent component of chilli peppers, was first isolated in 1876[1] and identified as *N*-(4-hydroxy-3-methoxybenzyl)-8-methylnon-6-eneamide in 1919.[2] Early structure–activity studies[3] established a basic picture of those features of the simple vanillylamide natural product which were important for pungency on the human tongue. Subsequent studies by Jancso-Gabor and Szolcsanyi[4,5] and, more recently, by workers at Procter and Gamble[6] further elaborated the SAR requirements in animal models for irritancy and analgesic activity, respectively. Over the last few years, we have established routine, quantitative, *in vitro* methods for measuring the effects of capsaicin analogues on cultures of dorsal root ganglion (DRG) neurons.[7] The measured effects are a consequence of excitation of these neurons by the agonist capsaicin or its analogues, *e.g.*, accumulation of $^{45}Ca^{2+}$ into DRG neurons. We have recently described SAR requirements for agonist activity in these cell-based assays[8-10] and established that agonist activity *in vitro* is predictive of antinociceptive activity *in vivo*. For convenience, the prototype agonist capsaicin, 1, was split up into three sections, whose structure–activity profiles were investigated in isolation. These structural sections were (1) the substituted aromatic ring, A-region, (2) the dipolar amide-bond region, B-region, and (3) the hydrophobic side chain, C-region. These regions are shown in Chart 1.

Chart 1

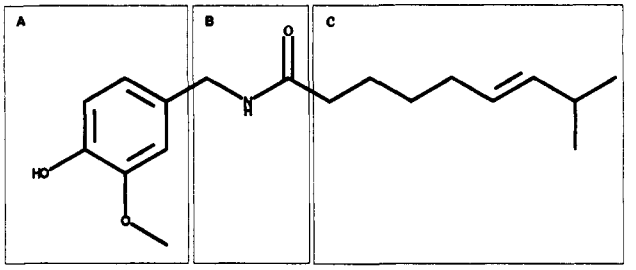

To date, however, antagonists based on the structure of capsaicin have not been described. Ruthenium red, a dye which is believed to block the capsaicin-operated channel, acts as a noncompetitive capsaicin antagonist. It also has a similar effect on various other channels, however. A selective, competitive antagonist at this receptor, which would be a novel pharmacological entity, would be of great interest.

There is now a large body of indirect evidence that capsaicin (and the highly potent diterpene resiniferatoxin, RTX) acts on a discrete receptor, unique to a subpopulation of primary afferent sensory neurons, which is intimately associated with (or intrinsic to) a novel ion channel which becomes permeant to cations on activation by an agonist.[7,11] This paper describes the discovery of capsazepine, the first competitive capsaicin antagonist,[12,13] which further strongly supports this hypothesis. Capsazepine has also been found to compete with [^{3}H]-resiniferatoxin binding in spinal cord, sensory neuron, and

† Preclinical Research, Sandoz AG, Basel.

• Abstract published in *Advance ACS Abstracts*, June 1, 1994.

0022-2623/94/1837-1942$04.50/0

Scheme 1

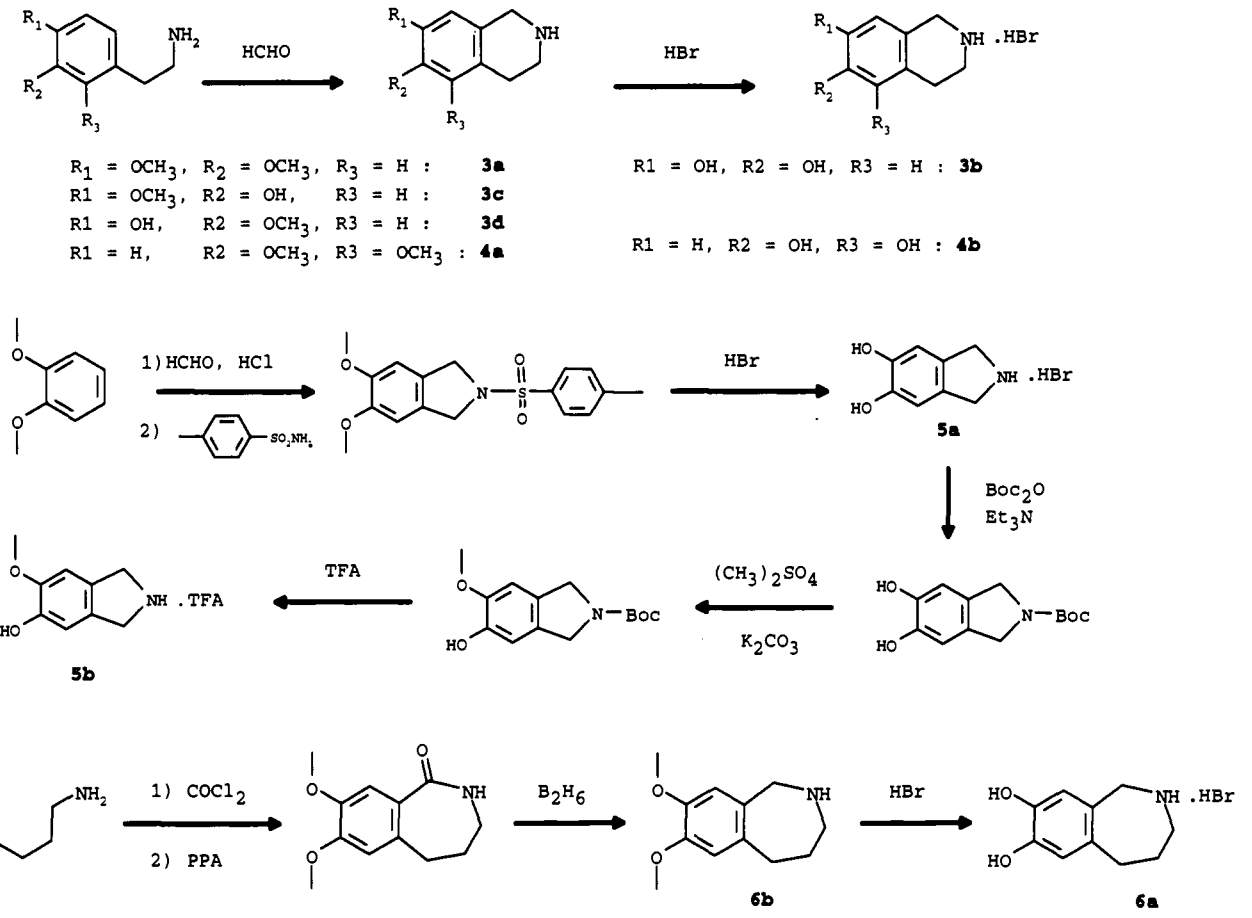

guinea pig airway membranes and appears to show differences in affinity for the receptor from these different tissue sources.[14] Two separate electrophysiological responses to capsaicin, a rapidly activating as well as a slowly activating current, both of which are blocked by capsazepine, have been reported in trigeminal ganglion neurons.[15] This may indicate the presence of more than one capsaicin receptor, although only one type of response (slowly activating) has been found in DRG neurons.[12,16]

Chemistry

2a was prepared by the method of Buckwalter and LaHann[17] by the reaction of vanillylamine hydrochloride with octyl isothiocyanate, in the presence of sodium hydroxide, in DMF. Compounds **2b,c** were prepared similarly using 4-chlorophenyl isothiocyanate and the appropriately substituted benzylamine.

Compounds **7a–d**, **8a,b**, **9a,b** and **10a,b** were prepared in a similar manner by reaction of the cyclic amines **3b–d**, **4b**, **5a,b**, and **6a,b**, respectively, with 4-chlorophenyl isothiocyanate or octyl isothiocyanate, as appropriate. The synthetic routes to these cyclic amines are shown in Scheme 1.

The six-membered cyclic amines (tetrahydroisoquinolines, THIQs) **3a–d** and **4a,b** were prepared by Pictet–Spengler cyclization of the appropriately substituted phenylethylamine in the presence of formaldehyde and demethylation, where appropriate, with HBr.

The five-membered cyclic amine (isoindoline) **5a** was prepared by the method of Ushujima *et al.*[18] by bischloromethylation of veratrole followed by condensation with *p*-toluenesulfonamide to give the N-protected dimethoxyisoindoline. N-Deprotection as well as demethylation was then effected with HBr. **5b** was prepared from **5a** by *N*-Boc protection with *tert*-butyl dicarbonate followed by monomethylation with dimethyl sulfate in the presence of K_2CO_3 and, finally, deprotection using TFA.

The seven-membered cyclic amines (benzazepines) **6a,b** were prepared from (3,4-dimethoxyphenyl)propylamine *via* the isocyanate by polyphosphoric acid-catalyzed cyclization yielding the intermediate benzazepinone. **6b** was prepared by B_2H_6 reduction of the benzazepinone, and the related **6a** was prepared by the demethylation of **6b** with HBr.

Biology

All compounds were tested as agonists in the Ca^{2+}-uptake assay.[7] Compounds which were full agonists or partial agonists with efficacy >50% were not tested as antagonists. Compounds which were inactive as agonists or were weak partial agonists (with efficacy <50%) were then tested as antagonists, using capsaicin as the reference agonist.

Results and Discussion

Structure–Activity Relationships. In a forthcoming publication,[19] we describe the way in which information gained from an exploration of structure–activity relationships in capsaicin agonists[8–10] led us to combine certain features of these molecules, resulting in highly potent agonists such as **2b** (Table 1). In such agonists, the substituted aromatic A-ring and the dipolar amide-bond B-region (Chart 1) are both highly sensitive to structural modification.[9,10] For example, the benzyl NH group in

Table 1. $^{45}Ca^{2+}$-Influx Activity of Unconstrained Thiourea Analogues

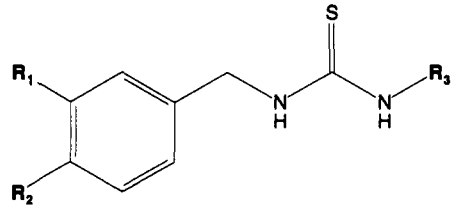

2

compound	R_1	R_2	R_3	Ca^{2+}-influx assay (μM) agonist EC_{50}	antagonist IC_{50}
1 (capsaicin)				0.30 ± 0.01	NT[a]
2a	OCH_3	OH	octyl	0.06 ± 0.01	NT
2b	OCH_3	OH	4-Cl-phenethyl	0.06 ± 0.01	NT
2c	OH	OH	4-Cl-phenethyl	0.10 ± 0.03	NT

[a] NT = not tested.

amides or thioureas (B-region functions which retain high activity) cannot be methylated without abolition of agonist activity in the Ca^{2+}-uptake assay. Furthermore, ring substituents in addition to the optimal 3,4-substituents invariably reduce or abolish activity.

It was interesting, therefore, that if the A-ring was constrained with respect to the B-region structures (such as thiourea), *e.g.*, by forming a THIQ ring, activity was retained. Since such constraint allows two possible positional isomers for the two oxygen functions which substitute the A-ring, both isomers were synthesized. In unconstrained agonist structures, it had previously been established that the 4-hydroxy, 3-methoxy substitution could be replaced by 3,4-dihydroxy (catechol) with retention of agonist activity[9] (compare **2b,c**, Table 1), and so, this substitution was adopted for reasons of synthetic ease.

Only one set of such compounds, those with the catechol function in the 6,7-position of the THIQ, **7a,b**, were active as agonists (Table 2; below). The isomeric 5,6-substituted compounds **8a,b** were inactive as agonists but were moderately potent *ant*agonists in the Ca^{2+}-uptake assay. These compounds were, however, highly unstable to aerobic oxidation, and antagonist activity was rapidly lost on storage of stock solutions of these compounds in DMSO

Chart 2

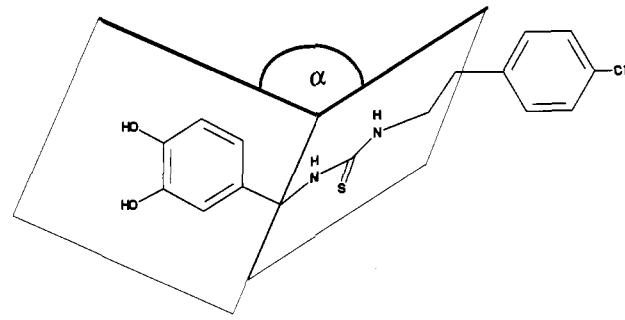

at 4 °C. No such instability was observed with the 6,7-substituted catechols.

The (4-chlorophenethyl)thioureas were found to be more potent than the *n*-octyl compounds with regard to both the agonist activity of **7a,b** as well as the *ant*agonist activity of the positional isomers **8a,b** and, so, were retained subsequently.

The apparent bioisosterism observed between the 3,4-catechols and the related 3-methyl ethers, mentioned above, was not so clear-cut in the constrained analogues. Substitution with a methyl group in either the 6- or 7-position of **7b** to give **7c,d** led to a retention of agonist potency and, in addition, to a reduction in efficacy in the calcium-influx assay. **7c**, as would be expected of a partial agonist, was active when tested in an antagonist paradigm. The positional isomer **7d** could not be similarly tested due to its relatively high intrinsic activity.

We have previously established that an sp^3-hybridized methylene unit between the A- and B-regions is critical for agonist activity.[10] We speculated that the role of this group is to act as a hinge between the A- and B-regions and that the THIQ analogues were active since they held these two units in an approximately coplanar disposition which is favorable for receptor activation. Nonconstrained compounds in which the benzylic N is alkylated by a simple methyl group are inactive,[10] perhaps since they cannot easily access this conformation, on steric grounds. In other words, we proposed that the angle between the plane of the thiourea and the plane of the ring (α, Chart 2) was

Table 2. $^{45}Ca^{2+}$-Influx Activity of Constrained Thiourea Analogues

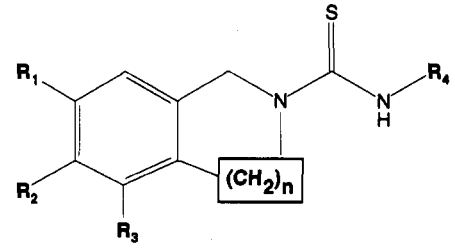

7-10

compound	R_1	R_2	R_3	R_4	*n*	Ca^{2+}-influx assay (μM) agonist EC_{50}	antagonist IC_{50}
7a	OH	OH	H	octyl	2	0.74 ± 0.06	NT
7b	OH	OH	H	4-Cl-phenethyl	2	0.29 ± 0.04	NT
7c	OCH_3	OH	H	4-Cl-phenethyl	2	1.09 ± 0.22[a]	1.23 ± 0.21
7d	OH	OCH_3	H	4-Cl-phenethyl	2	1.23 ± 0.36[b]	NT
8a	H	OH	OH	octyl	2	>100	3.48 ± 1.11[c]
8b	H	OH	OH	4-Cl-phenethyl	2	>100	0.44 ± 0.01[c]
9a	OH	OH	H	4-Cl-phenethyl	1	0.55 ± 0.08	NT
9b	OCH_3	OH	H	4-Cl-phenethyl	1	>100	>100
10a	OH	OH	H	4-Cl-phenethyl	3	>100	0.420 ± 0.046
10b	OCH_3	OCH_3	H	4-Cl-phenethyl	3	>100	6.99 ± 1.65

[a] Partial agonist, efficacy 18%. [b] Partial agonist, efficacy 41%. [c] Compounds highly sensitive to aerial oxidation.

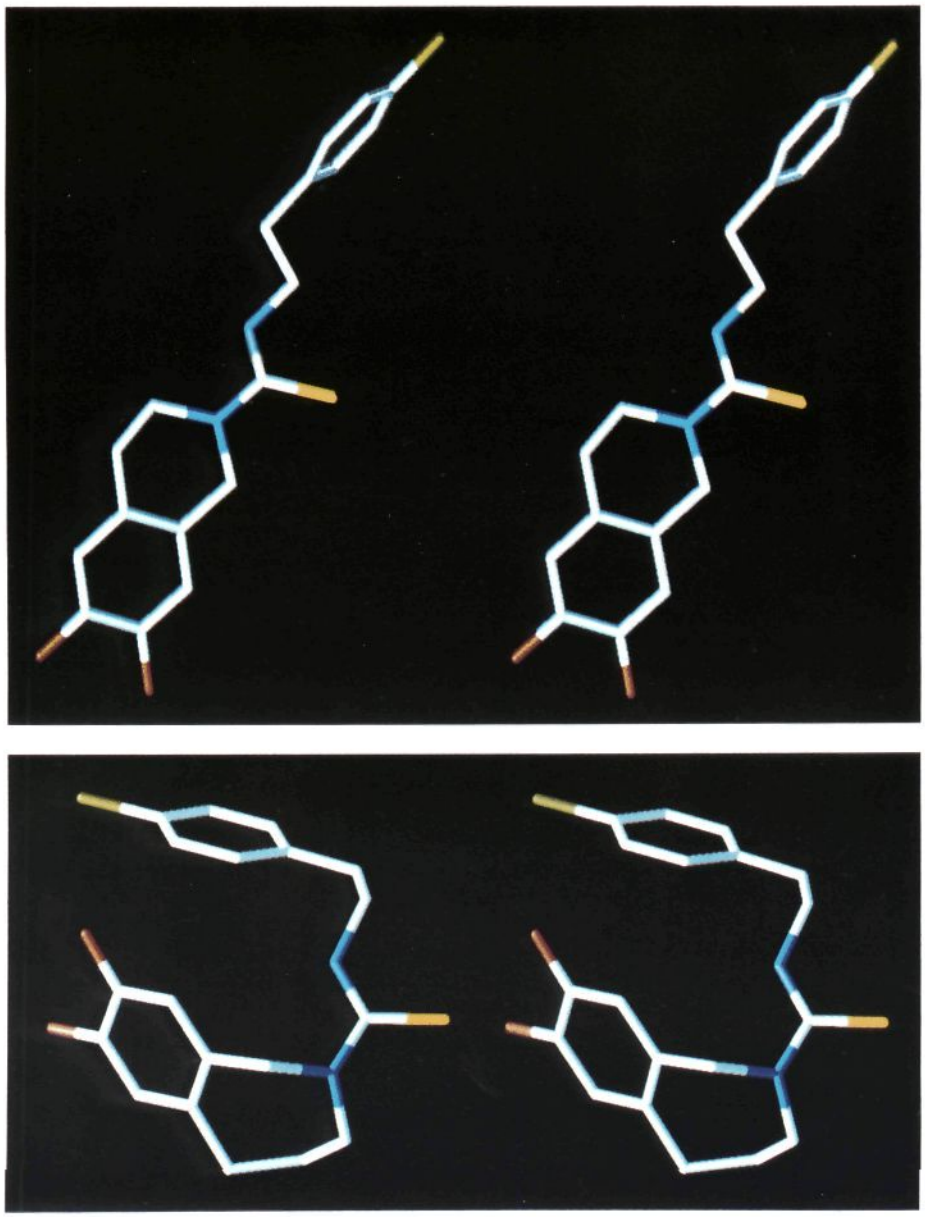

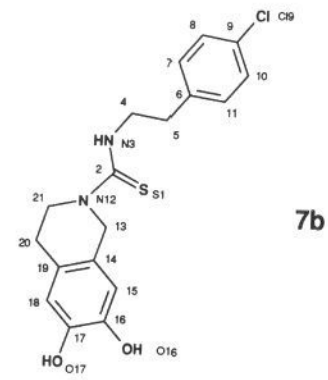

7b

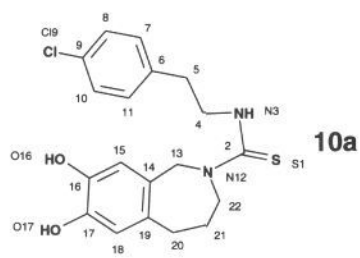

10a

Figure 1. Stereoviews (crossed) of X-ray crystal structures showing atom numbering for **7b** (top) and **10a** (bottom).

critical for agonist activity. Since we did not know the optimal value of this angle for activity, synthesis of a series of compounds, in which this angle was varied, was undertaken.

A series of analogues was synthesized in which the A- and B-regions were constrained by saturated ring systems of different sizes, varied between five and seven. Interestingly, compounds incorporating five- and six-membered ring constraints, *e.g.*, **9a** and **7b**, respectively, retained agonist activity and a similar level of potency to those of their unconstrained counterparts. A compound with a seven-membered constraint (the benzazepine, capsazepine, **10a**), however, was totally inactive in agonist assays but was a moderately potent antagonist. The observed antagonism was found to be competitive in a number of assay systems against both capsaicin and resiniferatoxin as reference agonists.[12] Schild plots with slopes close to unity were obtained in both cases. (capsaicin as agonist: $^{86}Rb^+$ efflux from DRG neurons, slope 1.09, K_d = 148 nM; [^{14}C]guanidinium efflux from vagus nerve, slope 1.09, K_d = 690 nM. RTX as agonist: accumulation of $^{45}Ca^{2+}$ into DRG neurons, slope 1.08, K_d = 220 nM; $^{86}Rb^+$ efflux from DRG neurons, slope 0.95, K_d = 107 nM.) Similar results have been obtained by other investigators.[13]

The dramatic change from agonist to antagonist on the formal addition of a single methylene group into the ring constraint in **7b** to give **10a** was striking. We therefore sought an explanation for the different pharmacological profile of these compounds which was based on the imposed conformational constraint. To this end, we obtained conformational data on these two compounds, a representative agonist and antagonist. X-ray crystal structures were obtained, the solution conformations of the compounds were studied by NMR spectroscopy, and the dynamic behavior of the molecules was simulated by molecular modeling techniques.

We were not able to crystallize the other antagonist, **8b**, and furthermore, its instability in solution made the study of solution conformation by NMR impracticable. Similar molecular modeling studies to those performed on **7b** and

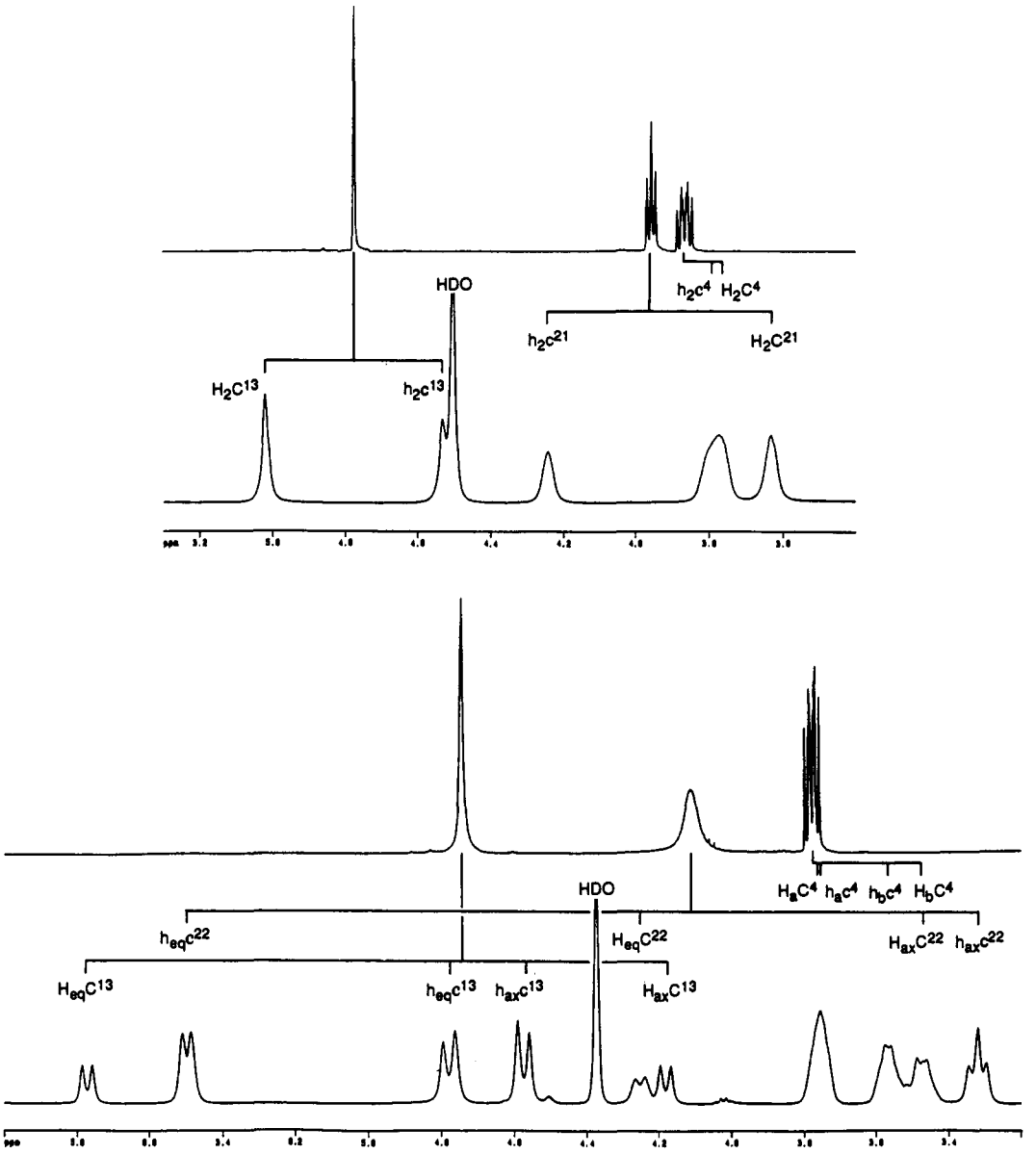

Figure 2. Comparison of the N–CH_2-region of the 1D ^1H NMR spectra of **7b** (top) and **10a** (bottom): top trace, room temperature spectra (301 K); lower trace, same region at 173 K. Uppercase letters refer to conformation I and lowercase letters to conformation II.

10a were, however, carried out to provide comparison of the conformational behavior of this compound with the other series.

Structure and Conformational Analysis. X-ray Crystallography. In the X-ray crystal structures of the agonist **7b** and the antagonist **10a**, the conformation of the saturated ring was found to be markedly different (Figure 1). In the six-membered-ring compound, **7b**, the saturated ring, and consequently the plane of the thiourea group, is virtually coplanar with repect to the A-ring (α = 163.6°, Chart 2) with only slight puckering of the bridging ethyl unit. By contrast, the benzazepine **10a**, capsazepine, exists in a pseudochair conformation in which the plane of the thiourea is approximately perpendicular to the plane of the aromatic ring (α = 93.5°). In both compounds, the thiourea exists in the (*E,Z*) configuration. The atomic numbering used in Figure 1 has been adopted throughout.

NMR Spectroscopy. At room temperature, 1D spectra of compounds **7b** and **10a** do not markedly differ except for the presence of the signal arising from the additional CH_2 group in the saturated ring. A single set of mostly sharp resonances indicates fast averaging between conformers. In **10a**, only the marked broadening of the H_2C^{22} signal reveals the existence of a dynamic process (*cf.* Figure 2). By lowering the temperature to 173 K, two well-separated sets of resonances corresponding to two conformers in slow exchange (further referred to as I and II) can be distinguished (Table 3).

Compound 7b. At room temperature, neither the two conformations nor any pair of the methylene protons give rise to separated resonances. At 173 K, however, a ratio of 60% vs 40% for conformers I and II, respectively, can be calculated from the signal integrals. These conformers differ remarkably in the resonance positions of all protons in the 4H-isoquinoline unit but mainly of HC^{13} and HC^{21} (Figure 2, top). In this six-membered-ring-constrained agonist, the pairs of methylene protons are still equivalent at 173 K. The marked broadening of the signals, however, indicates an intermediate exchange condition for the puckering motion of the aliphatic ring.

In the ROESY spectrum, an intense cross-peak indicating spatial proximity between HC^{21} and N^3H is visible in

Table 3. ^{1}H NMR Chemical Shift Values (ppm) for **7b** and **10a** in $(CD_3)_2CO$ at 301 and 173 K

	7b			10a		
	301 K	173 K, I (*Z,Z*), 60%	173 K, II (*E,Z*), 40%	301 K	173 K, I (*Z,Z*), 31%	173 K, II (*E,Z*), 69%
H–N^3	7.08	7.73	7.80	6.79	7.55	7.59
H$_b$–C^4	3.86	3.77	3.77	3.77	3.47	3.57
H$_b$–C^5	2.96	2.92	2.93	2.89	2.75	2.75
H–C^{7,11}	7.26	7.35	7.33	7.18	7.20	7.33
H$_{eq}$–C^{13}	4.77	5.02	4.53	4.74	5.77	4.78
H$_{ax}$–C^{13}	4.77	5.02	4.53	4.74	4.18	4.57
H–C^{15}	6.66	6.78	6.58	6.92	7.01	7.18
H–O^{16}	7.81	9.21	8.98	7.62	8.83	8.70
H–O^{17}	7.79	8.92	9.17	7.75	8.75	9.15
H$_{eq}$–C^{20}	2.74	2.78	2.70	2.80	2.75	2.75
H$_{ax}$–C^{20}	2.74	2.78	2.70	2.80	2.97	3.06
H$_{eq}$–C^{21}	3.96	3.63	4.24	1.75	1.74	1.81
H$_{ax}$–C^{21}	3.96	3.63	4.24	1.75	1.42	1.67
H$_{eq}$–C^{22}				4.11	4.25	5.50
H$_{ax}$–C^{22}				4.11	3.47	3.32

form I and, conversely, between HC^{13} and N^{3}H in form II (*cf.* Figure 3, top). The presence of strong exchange peaks between resonances of one proton in its two conformations reflects still noticeable interconversion between these forms. On the other hand, the puckering of the aliphatic ring is remarkably fast, since axial and equatorial protons of the three CH_2 groups are not distinguishable.

Compound 10a. As in the agonist **7b**, two different conformations are only visible at lowered temperature (173 K). The ratio between the corresponding forms I and II of the antagonist is calculated as 31% vs 69%. In **10a**, however, the seven-membered ring is rigid enough to make the two protons of each ring CH_2 group magnetically nonequivalent (MNE) (Figure 2, bottom). This MNE is remarkably large for only one CH_2 group in each conformer, namely for HC^{13} in I ($\Delta\delta_{eq-ax}$ = 1.59 ppm) and HC^{22} in II ($\Delta\delta_{eq-ax}$ = 2.18 ppm).

As for **7b**, a ROESY cross-peak connects N^{3}H and HC^{22} in form I and N^{3}H and HC^{13} in form II (*cf.* Figure 3, bottom). The absence of exchange peaks in the ROESY spectrum indicates that the interconversion between forms I and II is now very slow.

Whereas at normal temperature the spectra of **7b** and **10a** are quite similar and do not disclose any remarkable features, lowering the temperature to 173 K reveals two distinct conformations. They differ most characteristically in the shifts of the two ring N^{12}CH$_2$ groups, one group being shifted upfield, the other one downfield. This reflects a rotation of the C=S group by ~180° about the C^2–N^{12} bond. Thus, form I corresponds to the (*Z,Z*) conformation, where the sulfur atom points toward the C^{13} protons which are markedly deshielded. In contrast, in form II corresponding to the (*E,Z*) conformation, the C^{21} or C^{22} protons (in **7b** or **10a**, respectively) are shifted downfield. (*Z,Z*) and (*E,Z*) conformations refer to the atoms (C^{21}:N^{12}:C^2:S^1, S^1:C^2:N^3:C^4) in compound **7b** and to (C^{22}:N^{12}:C^2:S^1, S^1:C^2:N^3:C^4) in compound **10a**.

In summarizing this NMR study, a number of observations can be made as follows:

1. In both compounds, the (*E,Z*) (as observed in the crystal structures) and (*Z,Z*) thiourea conformations are populated to approximately equal extents.

2. Different thiourea conformations, however, are preferred in the two analogues. While the (*Z,Z*) form I is the major component for **7b**, for **10a**, it is the (*E,Z*) form II. Very different rates of exchange between thiourea conformers are apparent from the observation of exchange peaks. It can be concluded that a rather rapid interconversion takes place in **7b** ($10\ s^{-1} < k < 400\ s^{-1}$; the upper limit given by the shift difference between corresponding peaks in forms I and II). In the spectra of **10a**, however, exchange peaks are completely missing, indicating a very slow rate of exchange (*i.e.*, $k < 1\ s^{-1}$).

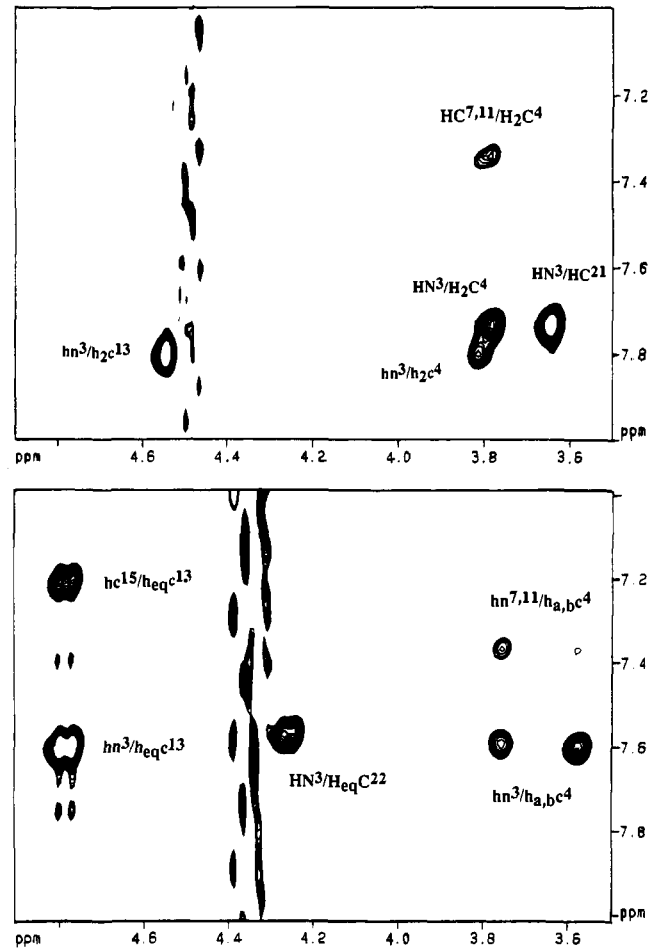

Figure 3. Part of contour plot of the ROESY spectra taken at 173 K showing the cross-peaks of N^{3}H to N^{12}CH$_2$ protons in **7b** (top) and **10a** (bottom). Uppercase letters refer to conformation I and lowercase letters to conformation II. For measuring conditions, see the Experimental Section.

3. Another difference exists in the unequal flexibility of the aliphatic rings. The coalescence of the CH_2 protons in the saturated ring of the THIQ moiety in **7b** implies a very fast flipping of the ring. On the other hand, in the seven-membered ring of **10a**, the axial and equatorial protons are magnetically nonequivalent, giving rise to distinct signals. Apparently, at low temperature, the saturated ring of the benzazepine unit adopts a specific shape with remarkable rigidity.

4. The conformation of the phenylethyl C-region group appears to be fairly random, and there are no notable differences between **7b** and **10a**. By contrast with the crystal structure of **10a**, there is no evidence from the NMR data for the close proximity of A-region and C-region aromatic rings.

Molecular Modeling. Molecular dynamics (MD) simulations (as described in the Experimental Section) were used to study the preferred conformations of the constraining saturated ring in the three analogues **7b**, **9a**, and **10a**. The five-membered-ring system in the compound **9a** was found to be coplanar with the catechol-ring moiety

Chart 3. Variation in Dihedral Angle α during Molecular Dynamics for **7b** (top) and **10a** (bottom)

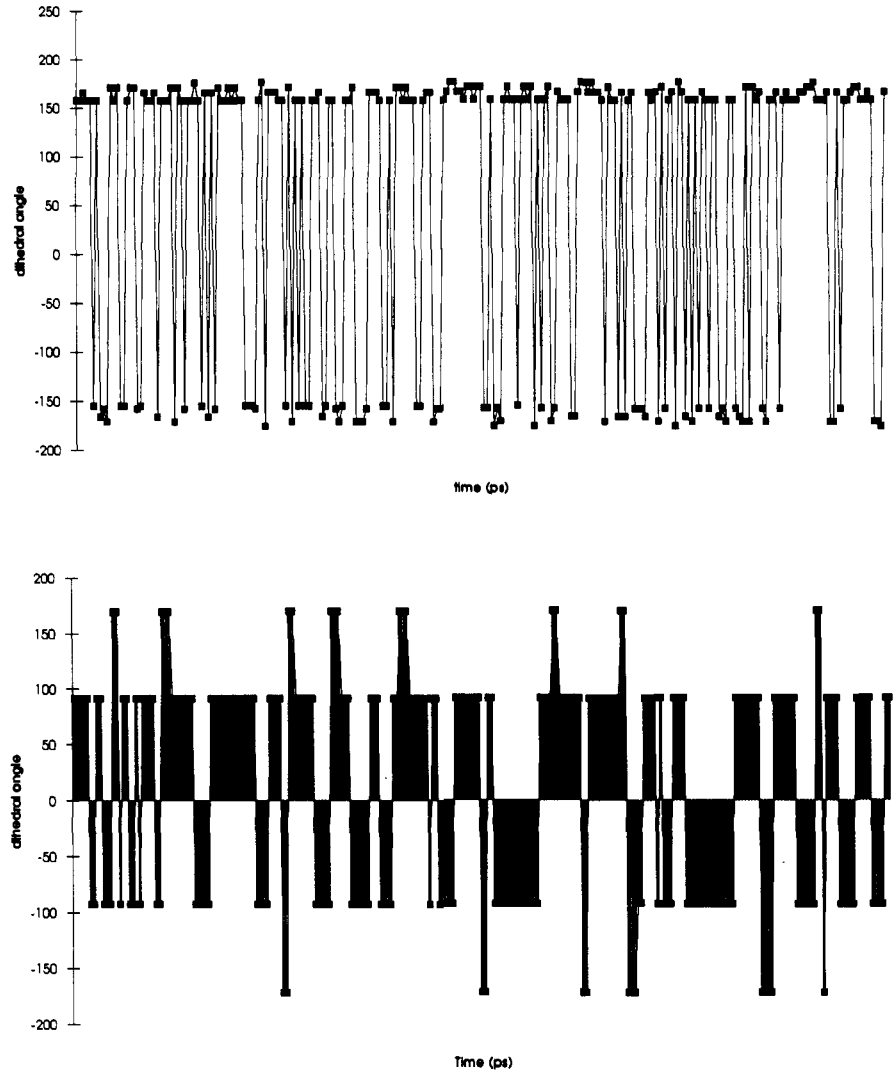

(A-region), whereas four discrete conformations of the seven-membered benzazepine ring in capsazepine, analogue **10a**, were identified and a range of conformations was shown to be available to the six-membered THIQ system in the compound **7b**.

The results from the modeling calculations are consistent with the experimentally derived X-ray and NMR data for compounds **7b** and **10a**. MD simulations clearly show that in the case of the THIQ system, **7b**, no single conformation of the saturated ring is favored. The plane that the thiourea moiety makes with the catechol ring (α, Chart 2) varies within a fairly tightly proscribed limit (180° ± 30°), resulting in a family of conformations which are all found to be populated (see Chart 3) and approximately equal in energy. This is indicative of the flexibility of the THIQ ring, in agreement with the observations by NMR of a very high ring-flip rate for the THIQ system. The X-ray crystal structure is very similar to the family of structures from the MD simulations, with the thiourea adopting a virtually coplanar arrangement with respect to the catechol ring, with only a slight puckering of the bridging ethylene unit (see Figure 4, top).

On the other hand, MD simulations on the benzazepine **10a** (capsazepine) were markedly different with only four discrete conformations accessible to the seven-membered ring (Chart 3). Over the 250-ps MD experiment, 92% of the conformations was found to be populated by the two pseudochair forms shown in Figure 4, bottom. One of these conformations was almost identical to the X-ray crystal structure of **10a** (α = 91.5°; structure shown in white), and the other is its near mirror image (α = −92.5°). Such behavior demonstrates the relative rigidity of this ring system in agreement with its solution behavior by NMR. The small population of more extended conformers are of significantly higher energy than the pseudochair forms. The lowest energy conformer of this type has an energy of 7 kcal mol^{-1} above the minimum-energy conformer found during MD.

The conformation of the thiourea B-region and the C-region side chain in compounds **9a**, **7b**, and **10a** was modeled using a systematic conformational search method as described in the Experimental Section. The energy difference between (*E*,*Z*) and (*Z*,*Z*) thiourea conformations was small, and both were populated to an approximately equal extent in all three analogues. This is in agreement with the NMR data presented on **7b** and **10a**. The aralkyl side chain in these compounds was similarly flexible with 30–40 qualitatively similar families of conformers populated in all three molecules.

The MD results with the THIQ antagonist **8b** were very similar to the other THIQ, **7b**, as would be expected.

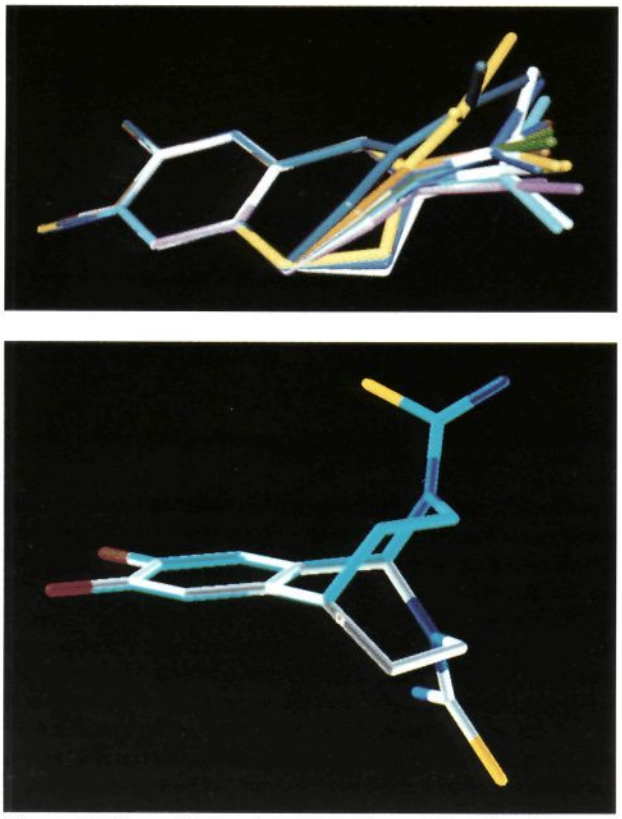

Figure 4. Accessible conformations from molecular dynamics simulations of **7b** (top) and **10a** (bottom). The C-region side chain has been omitted for clarity.

Conclusion

Three possible explanations for the different pharmacological profiles of **7b** and **10a** can be proposed.

1. The dramatic change in the relative disposition of the B- and C-regions with respect to that of the A-ring allows different H-bonding/hydrophobic contacts with receptor in the two compounds. The approximately planar structure of **7b** more closely resembles the conformation that unconstrained analogues must adopt for agonist activity than does that of **10a**.

2. The position of the (*E*/*Z*) thiourea equilibrium dictates agonism or antagonism. Different interactions with the receptor may be possible for the two conformations.

3. The greater conformational flexibility observed in the NMR spectrum and calculated for **7b** more closely resembles the behavior of unconstrained agonists at the receptor. **10a**, being relatively rigid, may still possess groups capable of imparting receptor affinity but cannot effect the conformational change induced by unconstrained agonists.

The second proposition is unlikely since both isomers are populated in both compounds, and so, the small changes in the ratios are unlikely to be of significance. Additionally, since the symmetrical five-membered-ring compound **9a**, in which the (*Z*,*Z*) and (*E*,*Z*) thiourea configurations are identical, is an agonist, antagonist activity must be dictated by some other feature.

The third proposition seems attractive since greater conformational rigidity is an explanation often advanced for the activity of antagonists.[20] However, since the saturated ring in the agonist **9a** must be completely rigid,

Chart 4

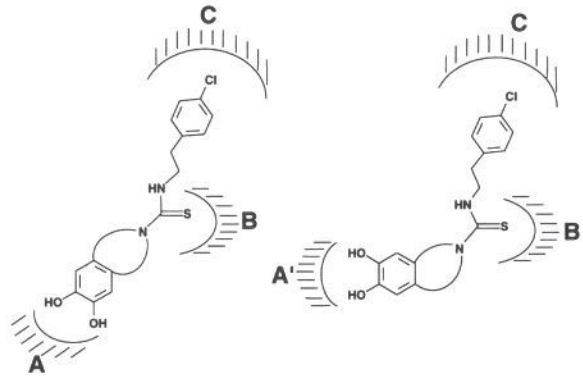

Agonist Binding Mode Antagonist Binding Mode

this feature cannot be solely responsible for the antagonist activity of **10a**. The structural feature which is responsible for this dramatic reversal in the pharmacological profile in these constrained analogues is most likely, therefore, to be the profoundly different disposition of the B-/C-regions with respect to that of the A-region in the two structures. The high stability of the pseudochair conformation into which the saturated ring is essentially "locked" does not allow the B-/C-regions to access the planar conformation with respect to the A-ring ($\alpha \sim 180°$), which we propose to be important for agonism in this series.

Conformational Rationale. A possible general explanation of the structural features which promote agonist or antagonist activity in these constrained capsaicin analogues is provided by consideration of the relative disposition of the three key pharmacophore groups, whose importance for activity has already been described.[8-10] These are (1) the A-region oxygen functions at the positions corresponding to 3 and 4 in the linear capsaicin analogues, (2) the B-region thiourea group, and (3) the aralkyl C-region.

Low-energy conformations of the various compounds, from the molecular dynamics calculations, are compared in Figure 5. The compounds **9a**, **7b**, **10a**, and **8b** are oriented such that the A-ring is in the plane of the paper and the thiocarbonyl moiety is horizontal. Within the limited series of compounds with ring constraints of different sizes, **9a**, **7b**, and **10a** (five-, six-, and seven-membered constraints, respectively), the angle α as defined in Scheme 1 defines the orientation of the catechol OH groups with respect to that of the thiocarbonyl group of the B-region and the C-region ring. These moieties in the antagonist **10a** have a distinctly "bent" disposition as compared to the nearly linear arrangement in the agonists **9a** and **7b**. In the THIQ compound **8b**, on the other hand, the different position of the ring O-substitution with repect to that in **7b** has the effect of making the disposition of the pharmacophores more similar to the antagonist **10a** than the agonists. A different binding mode for agonists and antagonists (Chart 4) can be hypothesized on the basis of these arguments.

This simple model provides a possible explanation for agonist and antagonist activity in these compounds. We are currently testing our hypothesis by the synthesis of a number of putative agonists and antagonists, as predicted by the model. Ultimately, this model should prove useful in guiding the design of second-generation, more potent capsaicin antagonists.

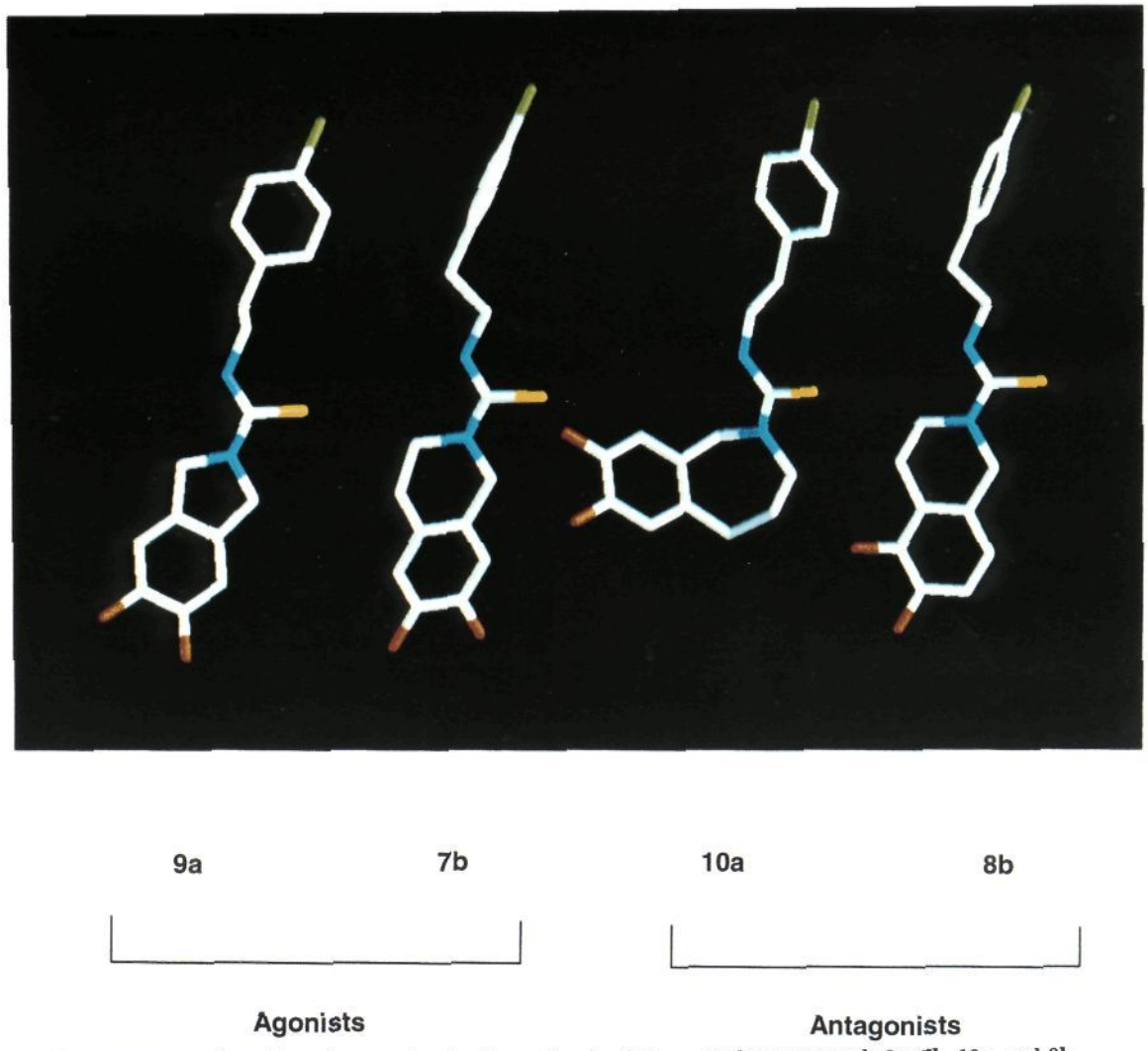

Figure 5. Low-energy conformations from molecular dynamics simulations on the compounds **9a**, **7b**, **10a**, and **8b**.

Experimental Section

Chemistry. General Information. Melting points were determined using a Reichert hot-stage microscope and are uncorrected. Routine NMR spectra were recorded using Hitachi-Perkin Elmer R12B and Varian Gemini 200 machines. High-field spectra were recorded using Varian VX400 400-MHz (University College London Chemistry Department) and Bruker AM500 500-MHz (Sandoz, Basel) instruments. All spectra were recorded using tetramethylsilane (TMS) as an internal standard, and chemical shifts are reported in parts per million (δ) downfield from TMS. Coupling constants are reported in hertz. A Perkin-Elmer 781 machine was used to record IR spectra. Elemental analyses were performed by the Analytical Department of University College London and were within 0.4% of theory. Mass spectra were recorded by the Mass Spectrometry Department of University College London, using a VG 7070F/H spectrometer and FAB spectra were recorded in Sandoz, Basel, using a VG 70-SE spectrometer. TLC was performed using Merck Kieselgel 60 F_{254} silica plates, and components were visualized using UV light and iodine vapor. HPLC was performed using a Waters 600 system (μ-Bondapak C-18 column (RP_{18}), using CH_3CN/0.1% aqueous TFA gradients of compositions stated in the text. Compounds were purified by flash column chromatography[21] using Merck Kieselgel 60 (230–400 mesh). Solvents were HLPC grade and were used without further purification. Solvents were dried according to the standard procedures.[22] Test compounds were homogenous by TLC or HPLC unless otherwise stated. Chemical yields were not optimized.

NMR Spectroscopy. For NMR measurements, 15 mg of the samples was dissolved in 0.5 mL of acetone-d_6 (Glaser, Basel). ^{1}H NMR spectra were recorded on a BRUKER AM 500 spectrometer. Chemical shift values are referred to internal TMS. For 1D spectra, eight scans of 16K time domain data points were acquired using a spectral width of 5 kHz and a repetition rate of 2.6 s. ROESY[23,24] spectra were recorded with a spectral width of 8065 Hz in ω_2 and ω_1 and the transmitter being placed downfield from the aromatic resonances. Sixteen scans of 512 increments corresponding to 31.7 ms in t_1 were acquired. In t_2, the acquisition time was 254 ms with a repetition time of 1.44 s. The mixing time was 150 ms at a spin–lock field of 38 kHz and a duty cycle delay of 12 μs, giving an effective field strength of 5.87 kHz. The data were processed on a BRUKER X32 workstation using UXNMR software. After zero-filling in ω_1 to give a matrix size of 4K × 1K and applying a cosine window function, the frequency domain spectrum was base-line corrected with a polynomial of third degree.

Molecular Modeling. Studies on the compounds **7b**, **9a**, and **10a** were performed on an Alliant Fx2800 computer using a Silicon Graphics workstation as the graphics display unit. The molecules were constructed using a proprietary modeling package, Draw, and the structures optimized using the algorithms of the molecular mechanics program Minimax.[25] The conformational space available to these three compounds was explored using MD simulations and a systematic incremental torsion angle approach. MD simulations were primarily used to study the conformation on the saturated ring, while the systematic search routine explored the conformational space available to the 4-chlorophenethyl side chain (the C-region). The MD simulations were accomplished using the Insight/Discover suite of programs.[26] Thus, each compound was submitted to the following protocol: A starting

structure was energy minimized using the CVFF force field and the conjugate gradient method until the rms derivative of the energy was below 0.01 kcal/mol/Å. The system was then brought to equilibrium, over 1 ps at a temperature of 300 K, before a molecular simulation study spanning a further 250 ps (at 300 K) was undertaken. Snap shots taken at 1-ps intervals were minimized using the optimization criteria outlined above. For each compound, the 251 resulting minimized structures were analyzed by superimposition of the catechol-ring moiety. The conformations accessible to the saturated ring system could then be easily analyzed.

A systematic conformational search algorithm encoded in the program Flexi[27] was used to study the conformational space available to the side chain. The lowest energy conformation from the MD simulation was used as a starting conformation for the systematic search. The five torsion angles connecting the C-region 4-chlorophenyl ring with the heterocyclic N atom were selected as active. The thioamide bonds were restricted to two conformations (0° and 180°), while the other three bonds were systematically rotated through 60°. Thus, each of the 864 starting conformations representing a regular grid in angle space was optimized using the BFGS minimizer encoded in the program Minimax. The resulting set of optimized structures represents the local minima on the energy hypersurface and clusters into a small number of family groups (see Results and Discussion).

Synthesis. *N*-(4-Hydroxy-3-methoxybenzyl)-*N'*-[(4-chlorophenyl)ethyl]thiourea[28] (2b). Vanillylamine hydrochloride (2.5 g, 13 mmol) was suspended in DMF (20 mL) and cooled on ice. NaOH (5.2 mL of 5 M solution, 26 mmol) was added, and the mixture was stirred for 15 min during which time a solution was obtained. 2-(4-Chlorophenyl)ethyl isothiocyanate (2.8 g, 14 mmol) in DMF (5 mL) was slowly added and the resulting soltuion stirred for 18 h. The crude product was obtained by dilution of the reaction mixture with water (250 mL) and extraction with diethyl ether (600 mL) in two portions. The ethereal extracts were combined and extracted with 1 M HCl, water, and finally brine, before drying over $MgSO_4$. Evaporation gave a white solid which was purified by recrystallization from aqueous MeOH to give a white crystalline solid, yield 2.19 g (48%): mp 143–144 °C; TLC (silica, CH_2Cl_2/MeOH 5:1) R_f 0.69; ^1H NMR (DMSO-d_6, 400 MHz) δ 2.82 (2H, t, J = 7.16 Hz, ArCH_2CH$_2$), 3.65 (2H, br m, ArCH$_2$CH_2N), 3.76 (3H, s, ArOCH$_3$), 4.52 (2H, br m, ArCH_2N), 6.73 (2H, m, ArH), 6.9 (1H, s, ArH), 7.26 (2H, d, J = 8.1 Hz, ArH), 7.36 (2H, d, J = 8.3 Hz, ArH), 7.40 (1H, br m, thiourea NH), 7.75 (1H, br m, thiourea NH), 8.90 (1H, s, ArOH); MS m/e 350 (M^+). Anal. ($C_{17}H_{19}N_2O_2ClS$) C, H, N.

***N*-(3,4-Dihydroxybenzyl)-*N'*-[(4-chlorophenyl)ethyl]thiourea (2c).** 2c was prepared as described for 2b from 3,4-dihydroxybenzylamine hydrobromide and 2-(4-chlorophenyl)-ethyl isothiocyanate and purified by recrystallization from CH_2Cl_2/hexane 1:1 to give a white solid, yield 63%: mp 101–105 °C; TLC (silica, CH_2Cl_2/MeOH 25:1) R_f 0.25; ^1H NMR (DMSO-d_6, 400 MHz) δ 2.80 (2H, t, J = 7.20 Hz, ArCH_2CH$_2$), 3.60 (2H, br m, ArCH$_2$CH_2N), 4.42 (2H, br m, ArCH_2N), 6.51 (1H, d of d, J = 8 Hz, J' = 2 Hz, ArH$_6$), 6.65 (1H, d, J = 8 Hz, ArH$_5$), 6.69 (1H, d, J' = 2 Hz, ArH$_2$), 7.26 (2H, d, J = 8.1 Hz, ArH), 7.36 (2H, d, J = 8.2 Hz, ArH), 7.40 (1H, br m, thiourea NH), 7.70 (1H, br m, thiourea NH), 8.75 (1H, s, ArOH), 8.85 (1H, s, ArOH); MS m/e 336 (M^+). Anal. ($C_{16}H_{17}N_2O_2ClS$·0.2H_2O) C, H, N.

6,7-Dihydroxy-1,2,3,4-tetrahydroisoquinoline Hydrobromide (3b). 6,7-Dimethoxy-1,2,3,4-tetrahydroisoquinoline hydrochloride (25.0 g, 91 mmol) was dissolved in 200 mL of 47–49% aqueous hydrobromic acid, and the mixture was refluxed for 24 h. The reaction was followed by ^1H NMR of aliquots from the reaction mixture until there was no signal at δ 3.8 corresponding to ArOCH$_3$. After cooling, the aqueous HBr was removed *in vacuo* to leave a brown residue. This was sonicated in 100 mL of MeOH, and the white solid was removed by filtration, washed with diethyl ether, and dried *in vacuo*, yield 19.81 g (74%): ^1H NMR (CD_3OD, 200 MHz) δ 2.95 (2H, t, J = 6.31 Hz, ArCH_2CH$_2$N), 3.43 (2H, t, J = 6.39 Hz, ArCH$_2$CH_2N), 4.18 (2H, s, ArCH$_2$N), 6.58 (1H, s, ArH), 6.62 (1H, s, ArH).

***N*-[(Octylamino)thiocarbonyl]-6,7-dihydroxy-1,2,3,4-tetrahydroisoquinoline (7a).** 6,7-Dihydroxy-1,2,3,4-tetrahydroisoquinoline hydrobromide, 3b (1.00 g, 4 mmol), and triethylamine (0.62 g, 6 mmol) were stirred in 75 mL of DMF (dried over 4A sieves) for 15 min. A solution of octyl isothiocyanate (0.68 g, 4 mmol) in 25 mL of dry DMF was added, and the reaction mixture was stirred for 24 h under N_2. After this time, the reaction was complete by TLC. The DMF was removed *in vacuo*, and the residue was suspended in 100 mL of H_2O and extracted with EtOAc (3 × 100 mL). The combined organic extracts were dried over Na_2SO_4 and filtered, and the solvent was removed *in vacuo*. The residue was purified by flash column chromatography (silica, CH_2Cl_2/MeOH 50:1) to leave a pale yellow oil, 1.2 g (80%): TLC (silica, CH_2Cl_2/MeOH 35:1) R_f 0.4; ^1H NMR (DMSO-d_6, 400 MHz] δ 0.88 (3H, t, J = 6.5 Hz, octyl CH$_3$), 1.2–1.4 (12H, env, octyl CH_2), 2.72 (2H, t, J = 5.81 Hz, ArCH_2CH$_2$N THIQ), 3.68 (2H, d of t, J = 6.5 Hz, J' = 8 Hz, NHCH_2CH$_2$), 3.78 (2H, t, J = 5.90 Hz, ArCH$_2$CH_2N THIQ), 4.75 (2H, s, ArCH_2N), 6.60 (1H, s, ArH), 6.65 (1H, s, ArH), 7.9 (1H, br s, CSNHCH$_2$), 8.9 (2H, br s, 2ArOH); MS m/e 336 (M^+); HPLC RP$_{18}$ (gradient 10–70% CH$_3$CN/0.1% aqueous TFA) >98% pure. Accurate mass calcd for $C_{18}H_{28}N_2O_2S$: 336.1871. Found: 336.1895.

***N*-[[[2-(4-Chlorophenyl)ethyl]amino]thiocarbonyl]-6,7-dihydroxy-1,2,3,4-tetrahydroisoquinoline (7b).** 6,7-Dihydroxy-1,2,3,4-tetrahydroisoquinoline hydrobromide, 3b (2.00 g, 8 mmol), and triethylamine (1.23 g, 12 mmol) were stirred in 75 mL of DMF (dried over 4A sieves) for 15 min. A solution of 2-(4-chlorophenyl)ethyl isothiocyanate (1.61 g, 8 mmol) in 25 mL of dry DMF was added, and the reaction mixture was stirred for 60 h under N_2. After this time the reaction was complete by TLC. The DMF was removed *in vacuo*, and the residue was suspended in 100 mL of H_2O and extracted with EtOAc (3 × 100 mL). The combined organic extracts were dried over Na_2SO_4 and filtered, and the solvent was removed *in vacuo*. The residue was purified by flash column chromatography (silica, CH_2Cl_2/MeOH 35:1) and the product crystallized from the eluant upon standing. The yellow crystals were collected by filtration and dried *in vacuo*, yield 2.5 g (86%): mp 164–166 °C; TLC (silica, CH_2Cl_2/MeOH 25:1) R_f 0.3; ^1H NMR (DMSO, 400 MHz) δ 2.65 (2H, t, J = 5.81 Hz, ArCH_2CH$_2$N THIQ), 2.88 (2H, t, J = 7.59 Hz, ArCH_2CH$_2$N), 3.70 (2H, t, J = 7.35 Hz, ArCH$_2$CH_2N), 3.87 (2H, t, J = 5.90 Hz, ArCH$_2$CH_2N THIQ), 4.68 (2H, s, ArCH_2N), 6.50 (1H, s, ArH), 6.55 (1H, s, ArH), 7.24 (2H, d, J = 8.4 Hz, 2ArH), 7.33 (2H, d, J = 8.4 Hz, 2ArH), 7.78 (1H, br s, CSNHCH$_2$), 8.75 (2H, br s, 2ArOH); FAB MS m/e 363 (MH^+). Anal. ($C_{18}H_{19}N_2O_2ClS$·0.4H_2O) C, H, N.

***N*-[[[2-(4-Chlorophenyl)ethyl]amino]thiocarbonyl]-7-methoxy-6-hydroxy-1,2,3,4-tetrahydroisoquinoline (7c).** 7c was prepared from 7-methoxy-6-hydroxy-1,2,3,4-tetrahydroisoquinoline, 3c,[29] and 2-(4-chlorophenyl)ethyl isothiocyanate, by the method described for the synthesis of 7b, and purified by flash column chromatography (silica, $CHCl_3$) to give a pale yellow solid, yield 45%: mp 149–150 °C; TLC (silica, CH_2Cl_2/MeOH 25:1) R_f 0.45; ^1H NMR (DMSO-d_6, 400 MHz) δ 2.70 (2H, t, J = 7.5 Hz, NHCH$_2$CH_2Ar), 2.90 (2H, t, J = 7.5 Hz, NHCH_2CH$_2$Ar), 3.70 (2H, t, J = 5.80 Hz, ArCH_2CH$_2$N THIQ), 3.75 (3H, s, ArOCH$_3$), 3.85 (2H, t, J = 5.80 Hz, ArCH$_2$CH_2N THIQ), 4.80 (2H, s, ArCH_2N THIQ), 6.60 (1H, s, ArH, THIQ), 6.70 (1H, s, ArH, THIQ), 7.30 (4H, m, ArH), 7.70 (1H, br t, NH), 8.82 (1H, br s, ArOH); MS m/e 376 (M^+). Anal. ($C_{19}H_{21}N_2O_2ClS$·0.3 H_2O) C, H, N.

***N*-[[[2-(4-Chlorophenyl)ethyl]amino]thiocarbonyl]-6-methoxy-7-hydroxy-1,2,3,4-tetrahydroisoquinoline (7d).** 7d was prepared from 6-methoxy-7-hydroxy-1,2,3,4-tetrahydroisoquinoline, 3d,[29] and 2-(4-chlorophenyl)ethyl isothiocyanate, by the method described for the synthesis of 7b, and purified by flash column chromatography (silica, $CHCl_3$) to give a pale yellow solid, yield 32%: mp 174–177 °C; TLC (silica, CH_2Cl_2/MeOH 20:1) R_f 0.6; ^1H NMR (DMSO-d_6, 400 MHz) δ 2.70 (2H, t, J = 7.5 Hz, NHCH$_2$CH_2Ar), 2.86 (2H, t, J = 7.5 Hz, NHCH_2CH$_2$Ar), 3.70 (2H, t, J = 5.90 Hz, ArCH_2CH$_2$N THIQ), 3.73 (3H, s, ArOCH$_3$), 3.90 (2H, t, J = 5.90 Hz, ArCH$_2$CH_2N THIQ), 4.70 (2H, s, ArCH_2N THIQ), 6.54 (1H, s, ArH, THIQ), 6.72 (1H, s, ArH, THIQ), 7.30 (4H, m, ArH), 7.75 (1H, br t, NH), 8.90 (1H, br s, ArOH); MS m/e 376 (M^+). Anal. ($C_{18}H_{21}N_2O_2ClS$) C, H, N.

5,6-Dihydroxy-1,2,3,4-tetrahydroisoquinoline Hydrobromide (4b). This compound was prepared from 5,6-dimethoxy-1,2,3,4-tetrahydroisoquinoline hydrobromide, 4a, by the method described for the preparation of 6,7-dihydroxy-1,2,3,4-tetrahy-

droisoquinoline hydrobromide, yield 89%: ^{1}H NMR (D_2O, 60 MHz) δ 2.70 (2H, t, J = 6.3 Hz, ArCH_2CH$_2$N), 3.25 (2H, t, J = 6.4 Hz, ArCH$_2$CH$_2$N), 4.0 (2H, s, ArCH$_2$N), 6.45 (1H, m, ArH), 6.52 (1H, m, ArH).

N-[(Octylamino)thiocarbonyl]-5,6-dihydroxy-1,2,3,4-tetrahydroisoquinoline (8a). This compound was prepared from 5,6-dihydroxy-1,2,3,4-tetrahydroisoquinoline hydrobromide, **4b**, and octyl isothiocyanate by the method described for the preparation of **7a**. The crude product was purified by flash column chromatography (silica, CH_2Cl_2/MeOH 50:1) to give a yellow oil, yield 80.4%: ^{1}H NMR (DMSO-d_6, 200 MHz) δ 0.88 (3H, t, J = 6.5 Hz, CH$_2$CH_3), 1.2–1.6 (12H, env, octyl CH_2), 2.73 (2H, t, J = 5.81 Hz, ArCH_2CH$_2$N THIQ), 3.46 (2H, d of t, J = 6.5 Hz, J' = 8 Hz, NHCH_2CH$_2$), 3.90 (2H, t, J = 5.90 Hz, ArCH$_2$CH_2N THIQ), 4.75 (2H, s, ArCH_2N), 6.42 (1H, d, J = 7.1 Hz, ArH), 6.62 (1H, d, J = 7.1 Hz, ArH), 7.58 (1H, br t, CSNHCH$_2$), 8.40 (1H, br s, ArOH), 9.1 (1H, br s, ArOH); FAB MS m/e 337 (MH$^+$); HPLC RP$_{18}$ (gradient 10–70% CH$_3$CN/0.1% aqueous TFA) >98% pure. Accurate mass calcd for $C_{18}H_{28}N_2SO_2$: 336.1871. Found: 336.1874.

N-[[[2-(4-Chlorophenyl)ethyl]amino]thiocarbonyl]-5,6-dihydroxy-1,2,3,4-tetrahydroisoquinoline (8b). This compound was prepared from 5,6-dihydroxy-1,2,3,4-tetrahydroisoquinoline hydrobromide, **4b**, and 2-(4-chlorophenyl)ethyl isothiocyanate by the method described for the preparation of **7b**. The crude product was purified by flash column chromatography (silica, CH_2Cl_2/MeOH 50:1), yield 43%: mp 151.5–153 °C; TLC (silica, CH_2Cl_2/MeOH 5:1) R_f 0.75; ^{1}H NMR (DMSO-d_6, 200 MHz) δ 2.73 (2H, t, J = 5.81 Hz, ArCH_2CH$_2$N THIQ), 2.92 (2H, t, J = 7.09 Hz, ArCH_2CH$_2$N), 3.74 (2H, d of t, J = 7.4 Hz, ArCH$_2$CH_2-NH), 3.90 (2H, t, J = 5.90 Hz, ArCH$_2$CH_2N THIQ), 4.83 (2H, s, ArCH_2N), 6.52 (1H, d, J = 7.1 Hz, ArH), 6.73 (1H, d, J = 7.1 Hz, ArH), 7.24 (2H, d, J = 8.4 Hz, 2ArH), 7.33 (2H, d, J = 8.4 Hz, 2ArH), 7.78 (1H, br t, CSNHCH$_2$), 8.75 (2H, br s, 2ArOH); FAB MS m/e 363 (MH$^+$). Anal. ($C_{18}H_{19}N_2O_2ClS$) C, H, N.

2-[[[2-(4-Chlorophenyl)ethyl]amino]thiocarbonyl]-5,6-dihydroxyisoindoline (9a). 5,6-Dihydroxyisoindoline hydrobromide, **5a**,[18] (330 mg, 1.4 mmol) was dissolved, with triethylamine (156 mg, 1.5 mmol), in DMF (5 mL), with stirring under N_2. After 15 min, a solution of 2-(4-chlorophenyl)ethyl isothiocyanate (281 mg, 1.4 mmol) in 5 mL of DMF was added. The solution was stirred at room temperature for 60 h. The DMF was removed *in vacuo*, and the residue was partitioned between EtOAc and water. The organic phase was dried over Na_2SO_4 and filtered, and the solvent was removed *in vacuo*. The residue was recrystallized from EtOAc/hexane, yield 485 mg (97%): mp 200–210 °C dec; TLC (silica, CH_2Cl_2/MeOH 10:1) R_f 0.44; ^{1}H NMR (DMSO-d_6, 400 MHz) δ 2.90 (2H, t, J = 7.51 Hz, ClArCH_2CH$_2$), 3.70 (2H, br m, ClArCH$_2$CH_2NH), 4.65 (4H, br s, 2ArCH$_2$N), 6.70 (2H, s, 2ArH), 7.25 (2H, d, J = 8.4 Hz, 2ArH), 7.34 (2H, d, J = 8.4 Hz, 2ArH), 7.45 (1H, br t, CH$_2$NHCS); MS m/e 349 (M$^+$). Anal. ($C_{17}H_{17}N_2O_2ClS$·0.5H$_2$O) C, H, N.

N-[(*tert*-Butyloxy)carbonyl]-5,6-dihydroxyisoindoline. 5,6-Dihydroxyisoindoline hydrobromide, **5a** (4.05 g, 17.5 mmol), was stirred in 50% aqueous dioxan (100 mL), under N_2, and triethylamine (3.3 mL, 19.2 mmol) was added. Di-*tert*-butyl dicarbonate (2.35 g, 10.8 mmol) in dioxan (25 mL) was added and the reaction mixture stirred for 18 h. After this time, the dioxan was removed *in vacuo*, water (100 mL) was added, and the solution was extracted with CH_2Cl_2. The organic phase was dried over Na_2SO_4 and evaporated to give a dark colored oil which was purified by flash column chromatography (silica, CH_2Cl_2/MeOH 10:1). The pure fractions yielded a colorless glass on evaporation, yield 2 g (46%): TLC (silica, CH_2Cl_2/MeOH 10:1) R_f 0.45; ^{1}H NMR (CDCl$_3$, 60 MHz) δ 1.5 (9H, s, *tert*-butyl-CH$_3$), 4.85 (4H, s, 2ArCH$_2$N), 6.7 (2H, s, ArH).

N-[(*tert*-Butyloxy)carbonyl]-5-hydroxy-6-methoxyisoindoline. *N*-[(*tert*-Butyloxy)carbonyl]-5,6-dihydroxyisoindoline (200 mg, 0.79 mmol) was dissolved in CH$_3$CN (3 mL), and potassium carbonate (220 mg, 1.59 mmol) was added and the suspension stirred under N_2. Dimethyl sulfate (50 mg, 0.40 mmol), in CH$_3$CN (3 mL), was slowly added, and the mixture was stirred, at reflux, for 2 h. After this time, the cooled suspension was filtered and the filtrate was evaporated *in vacuo*, leaving a brown oil which was purified by flash column chromatography (silica, cyclohexane/EtOAc 5:1). The pure fractions yielded a colorless glass on evaporation, yield 160 mg (76%): TLC (silica, CH_2Cl_2/MeOH 20:1) R_f 0.55; ^{1}H NMR (CDCl$_3$, 60 MHz) δ 1.5 (9H, s, *tert*-butyl-CH$_3$), 3.90 (3H, s, ArOCH$_3$), 4.60 (4H, s, 2ArCH$_2$N), 5.7 (1H, br s, ArOH), 6.8 (2H, s, ArH).

2-[[[2-(4-Chlorophenyl)ethyl]amino]thiocarbonyl]-5-hydroxy-6-methoxyisoindoline (9b). N-[(*tert*-Butyloxy)carbonyl]-5-hydroxy-6-methoxyisoindoline (0.8 g, 3 mmol) was dissolved in CH_2Cl_2 (75 mL), and trifluoroacetic acid (3 mL, 39 mmol) was added. The reaction mixture was then stirred for 18 h after which time no starting material remained by TLC. The solvent was removed *in vacuo*, leaving a dark solid, 670 mg. The crude deprotected product, **5b**, without purification, was dissolved in THF (30 mL), and triethylamine (450 mg, 4.5 mmol) was added and the solution stirred under N_2. 2-(4-Chlorophenyl)ethyl isothiocyanate (0.60 g, 3 mmol), as a solution in THF (20 mL), was slowly added. The reaction mixture was stirred for 18 h before removal of the solvent *in vacuo*, leaving a brown solid which was purified by flash column chromatography (silica, cyclohexane/EtOAc 2:1). Evaporation of the pure fractions gave a white solid, yield 0.45 g (41%): mp 210–212 °C; TLC (silica, CH_2Cl_2/MeOH 50:1) R_f 0.48; ^{1}H NMR (DMSO-d_6, 400 MHz) δ 2.88 (2H, t, J = 7.49 Hz, ClArCH_2CH$_2$), 3.70 (2H, br m, ClArCH$_2$CH_2NH), 3.77 (3H, s, ArOCH$_3$), 4.68 (4H, br s, 2ArCH$_2$N), 6.73 (1H, s, ArH), 6.90 (1H, s, ArH), 7.27 (2H, d, J = 8.5 Hz, 2ArH), 7.34 (2H, d, J = 8.5 Hz, 2ArH) , 7.51 (1H, br t, CH$_2$NHCS), 8.96 (1H, br s, ArOH); MS m/e 363 (M$^+$). Anal. ($C_{18}H_{19}N_2O_2ClS$) C, H, N.

3-(3,4-Dimethoxyphenyl)propyl Isocyanate. 3-(3,4-Dimethoxyphenyl)propylamine hydrochloride (32.0 g, 138 mmol) was suspended and stirred in 150 mL of toluene; 80 mL of 20% phosgene in toluene (16.0 g, 152 mmol) was slowly added. The reaction mixture was heated to 100 °C, with exhaust gases from the top of the condenser bubbled through 5 M NaOH(aq). After 90 min, a further 80 mL of the phosgene solution was added; after 60 min, another 50 mL was added. Fifteen minutes later, the reaction mixture was entirely in solution. After an hour, the temperature was raised to 140 °C and half the toluene, as well as any remaining phosgene, was distilled into 5 M NaOH(aq). The remaining toluene was removed *in vacuo* and the isocyanate purified by flash column chromatography (silica, cyclohexane/EtOAc 2:1) to give a pale yellow oil, yield 20.0 g (66%): TLC (silica, cyclohexane/EtOAc 1:1) R_f 0.52; IR ν = 2270 cm^{-1}; ^{1}H NMR (CDCl$_3$, 200 MHz) δ 1.88 (2H, m, ArCH$_2$CH_2CH$_2$NCO), 2.65 (2H, t, J = 7.47 Hz, ArCH_2CH$_2$CH$_2$NCO), 3.28 (2H, t, J = 6.53 Hz, ArCH$_2$CH$_2$CH_2NCO), 3.84 (3H, s, ArOCH$_3$), 3.85 (3H, s, ArOCH$_3$), 6.75 (3H, m, 3ArH).

7,8-Dimethoxy-2,3,4,5-tetrahydro-2-benzazepin-1-one. Polyphosphoric acid (130 g) was heated until it was easy to stir (90 °C), at which time 3-(3,4-dimethoxyphenyl)propyl isocyanate (20 g, 90 mmol) was added slowly, such that the temperature never exceeded 110 °C. The reaction mixture was stirred for 90 min at 110 °C, allowed to cool slowly to room temperature, and, then, cooled to below 0 °C on a salt/ice bath. 5 M NaOH(aq) was gradually added, so that the temperature never exceeded 120 °C, until the reaction mixture had a pH value approaching 9. After the addition of 200 mL of dichloromethane, a dense white precipitate formed, which was eventually dissolved when diluted with 5 L of water. This was extracted with CH_2Cl_2; the organic phase was dried over Na_2SO_4 and filtered, and the solvent was removed *in vacuo*. The compound was purified by flash column chromatography (silica, CH_2Cl_2/MeOH 25:1) and recrystallized from EtOAc, yield 7.91 g (40%): mp 182–183 °C; TLC (silica, CH_2Cl_2/MeOH 10:1) R_f 0.50; ^{1}H NMR (CDCl$_3$, 200 MHz) δ 2.02 (2H, m, ArCH$_2$CH_2CH$_2$), 2.82 (2H, t, J = 7.15 Hz, ArCH_2CH$_2$), 3.15 (2H, q, J = 6.38 Hz, CH$_2$CH_2NH), 3.92 (3H, s, ArOCH$_3$), 3.93 (3H, s, ArOCH$_3$), 6.69 (1H, s, ArH), 6.97 (1H, br t, NH), 7.27 (1H, s, ArH); MS m/e 221 (M$^+$). Anal. ($C_{12}H_{15}NO_3$) C, H, N.

7,8-Dimethoxy-2,3,4,5-tetrahydro-2-benzazepine (6b). 7,8-Dimethoxy-2,3,4,5-tetrahydro-2-benzazepin-1-one (5.01 g, 22.7 mmol) was dissolved in 50 mL of anhydrous THF under N_2 with stirring on ice, and 1 M diborane in THF (50 mL) was added dropwise. The solution was then heated to reflux and refluxed for 15 h. The solution was cooled to 0 °C on an ice/salt bath, and methanol (80 mL) was added. Once the solution had cooled to 0 °C, 2 M HCl(aq) (200 mL) was added dropwise; the solution was heated to 80 °C and stirred for 2 h. After cooling to room

temperature, the THF and MeOH were removed *in vacuo*. The compound was purified by flash column chromatography (silica, methanol), yield 3.5 g (75%): TLC (silica, methanol) R_f 0.08; ^{1}H NMR ($CDCl_3$, 200 MHz) δ 1.17 (2H, m, $ArCH_2CH_2CH_2$), 2.90 (2H, m, $ArCH_2CH_2$), 3.20 (2H, m, CH_2CH_2NH), 3.49 (1H, m, CH_2NHCH_2), 3.86–3.88 (8H, m, overlapping $2ArOCH_3$ and $ArCH_2NH$), 6.68 (1H, s, ArH), 6.70 (1H, s, ArH); MS *m/e* 207 (M^+).

7,8-Dihydroxy-2,3,4,5-tetrahydro-2-benzazepine Hydrobromide (6a). This compound was prepared from 7,8-dimethoxy-2,3,4,5-tetrahydro-2-benzazepine, **6b** (3.5 g, 16.9 mmol), as described for 6,7-dihydroxy-1,2,3,4-tetrahydroisoquinoline hydrobromide, yield 2.53 g (58%): TLC (silica, CH_2Cl_2/MeOH/acetic acid 120:90:5) R_f 0.70; ^{1}H NMR (CD_3OD, 200 MHz) δ 1.91 (2H, m, $ArCH_2CH_2CH_2$), 2.88 (2H, m, $ArCH_2CH_2$), 3.42 (2H, m, CH_2CH_2NH), 4.21 (2H, s, $ArCH_2NH$), 6.69 (1H, s, ArH), 6.80 (1H, s, ArH).

***N*-[[[2-(4-Chlorophenyl)ethyl]amino]thiocarbonyl]-7,8-dihydroxy-2,3,4,5-tetrahydrobenzazepine (10a).** 7,8-Dihydroxy-2,3,4,5-tetrahydro-2-benzazepine hydrobromide, **6a** (2.53 g, 9.7 mmol), was suspended in 50 mL of THF, with triethylamine (1.46 g, 14.4 mmol), and the mixture was stirred for 20 min. A solution of 2-(4-chlorophenyl)ethyl isothiocyanate (1.81 g, 9.7 mmol) in 50 mL of dry THF was added and the mixture stirred for 15 h. The reaction was incomplete by TLC, so a further 750 mg of triethylamine was added and the reaction stirred for a further 3 h. The THF was removed *in vacuo*, and the residue was partitioned between EtOAc and water. The organic phase was dried over Na_2SO_4 and filtered, and the solvent was removed *in vacuo*. The compound was purified by flash column chromatography (silica, CH_2Cl_2/MeOH 25:1) and recrystallized from EtOAc/*n*-hexane, yield 2.88 g (79%): mp 157–158 °C; TLC (silica, CH_2Cl_2/MeOH 10:1) R_f 0.55; ^{1}H NMR (DMSO-d_6, 400 MHz) δ 1.65 (2H, br m, $ArCH_2CH_2CH_2$), 2.70 (2H, m, $ClArCH_2CH_2$), 2.80 (2H, t, J = 7.63 Hz, $ArCH_2CH_2CH_2$), 3.60 (2H, m, $ArCH_2CH_2CH_2N$), 3.98 (2H, m, $ClArCH_2CH_2NH$), 4.68 (2H, m, $ArCH_2N$), 6.55 (1H, s, ArH), 6.86 (1H, s, ArH), 7.25 (2H, d, J = 8.4 Hz, 2ArH), 7.34 (2H, d, J = 8.4 Hz, 2ArH), 7.48 (1H, br t, NH); MS *m/e* 376 (M^+). Anal. ($C_{19}H_{21}N_2O_2ClS$) C, H, N.

***N*-[[[2-(4-Chlorophenyl)ethyl]amino]thiocarbonyl]-7,8-dimethoxy-2,3,4,5-tetrahydrobenzazepine (10b).** **10b** was prepared by the method described for **10a** from 7,8-dimethoxy-2,3,4,5-tetrahydro-2-benzazepine, **6b**, yield 65.4%: mp 157–158 °C; TLC (silica, cyclohexane/EtOAc 1:1) R_f 0.40; ^{1}H NMR ($CDCl_3$, 200 MHz) δ 1.85 (2H, m, $ArCH_2CH_2CH_2$), 2.84–2.91 (4H, m, $ArCH_2CH_2$ and $ArCH_2CH_2$, benzazepine), 3.78 (3H, s, $ArOCH_3$), 3.87 (3H, s, $ArOCH_3$), 3.88 (2H, m, CH_2CH_2NH), 4.12 (2H, m, CH_2CH_2NH), 4.62 (2H, s, $ArCH_2NH$), 5.37 (1H, br t, NH), 6.57 (1H, s, ArH), 6.69 (1H, s, ArH), 7.15 (2H, d, J = 8.2 Hz, 2ArH), 7.24 (2H, d, J = 8.2 Hz, 2ArH); MS *m/e* 405 (M^+). Anal. ($C_{21}H_{25}N_2O_2ClS$) C, H, N.

Biology. *In vitro* assay—$^{45}Ca^{2+}$ Uptake. The uptake and accumulation of $^{45}Ca^{2+}$ by capsaicin analogues was studied in neonatal rat cultured spinal sensory neurons by the method described in detail by Wood *et al.*[7] In brief, spinal (dorsal root) ganglia were dissected aseptically from newborn rats and incubated sequentially at 37 °C for 30 min with collagenase (Boeringer Mannheim) followed by 30 min in 2.5 mg/mL trypsin (Worthington), both enzymes made up in Ham's F-14 medium. The ganglia were then washed in medium supplemented with 10% horse serum and the cells dissociated by trituration through a Pasteur pipette. The cells were collected by centrifugation and resuspended in Ham's F-14 medium with 10% horse serum plus 1 μg/mL nerve growth factor. The neuronal preparation was plated onto poly(D-ornithine) Terasaki plates (Flow Laboratories) at a density of 1000 neurons/well. Cultures were incubated at 37 °C in a humidified incubator gassed with 3% CO_2 in air. After the cells had adhered, 10^{-4} M cytosine arabinoside, a mitotic inhibitor, was added to the culture for 48 h to kill the dividing non-neuronal cells.

$^{45}Ca^{2+}$-uptake assays were made on 3–7-day-old cultures. The Terasaki plates were washed four times with calcium-free Hank's balanced salt solution (BSS) buffered with 10 mM HEPES (pH 7.4). Excess medium was drained from the plate and then 10 μL of remaining medium removed from the individual wells. For agonist studies, 10 μL of medium containing the test concentration of compound plus 10 μCi/mL $^{45}Ca^{2+}$ (Amersham) was added to each well. For antagonist studies, the added medium contained $^{45}Ca^{2+}$ and 0.5 μM capsaicin together with the test concentration of compound. All media contained 1% dimethyl sulfoxide (DMSO) to keep the compounds in solution. The neurons were incubated at room temperature for 10 min, and then the Terasaki plates were washed six times in BSS and dried in an oven; 10 μL of 0.3% sodium dodecyl sulfate was added to each well to dissolve the cells and extract the $^{45}Ca^{2+}$. The contents of each well were transferred to scintillation vials and counted in 1 mL of Beckman CP scintillation fluid. In all experiments, one group of replicates was treated with medium alone to estimate the background uptake.

EC_{50} (the concentration of drug necessary to produce 50% of the maximal response) and IC_{50} values (the concentration of drug necessary to reduce the response to 0.5 μM capsaicin by 50%) were estimated with at least six replicates at each concentration. Each compound was tested in two or more independent experiments. Agonist data (1) and antagonist data (2) were fitted with a sigmoidal functions of the form:

$$(1)\ \text{total uptake} = a/(1 + (EC_{50}/\text{conc})^b) + c$$

$$(2)\ \text{total uptake} = a[1 - 1/(1 + (IC_{50}/\text{conc})^b)] + c$$

where

a = the maximum evoked uptake

b = the slope factor

c = the background uptake in the absence of compound.

Results are given as mean ± SEM.

Supplementary Material Available: Synthetic methods for the preparation of three compounds whose preparations (by other routes) have been previously published and X-ray crystallographic data for compounds **7b** and **10a** (10 pages). Ordering information is given on any current masthead page.

References

(1) Thresh, M. *Pharm. J.* **1876**, 7.
(2) Nelson, E. K. The Constitution of Capsaicin, the Pungent Principle of Capsicum. *J. Am. Chem. Soc.* **1919**, *41*, 1115–1472.
(3) Jones, E. C. S.; Pyman, F. L. The Relation Between Chemical Constitution and Pungency in Acid Amides. *J. Chem. Soc.* **1925**, *127*, 2588–2598.
(4) Szolcsanyi, J.; Jansco-Gabor, A. Sensory Efects of Capsaicin Congeners I. Relationship between Chemical Structure and Pain-producing Potency of Pungent Agents. *Arzneim.-Forsch.* **1975**, *25*, 1877–1881.
(5) Szolcsanyi, J.; Jansco-Gabor, A. Sensory Effects of Capsaicin Congeners II. Importance of Chemical Structure and Pungency in Desensitising Activity of Capsaicin-type Compounds. *Arzneim.-Forsch.* **1976**, *26*, 33–37.
(6) Janusz, J. M.; Buckwalter, B. L.; Young, P. A.; LaHann, T. R.; Farmer, R. W.; Kasting, G. B.; Loomans, M. E.; Kerckaert, G. A.; Maddin, C. S.; Berman, E. F.; Bohne, R. L.; Cupps, T. L.; Milstein, J. R. Vanilloids. 1. Analogues of Capsaicin with Antinociceptive and Antiinflammatory Activity. *J. Med. Chem.* **1993**, *36*, 2595–2604.
(7) Wood, J. N.; Winter, J.; James, I. F.; Rang, H. P.; Yeats, J.; Bevan, S. Capsaicin-induced Ion Fluxes in Dorsal Root Ganglion Cells in Culture. *J. Neurosci.* **1988**, *8*, 3208–3220.
(8) Walpole, C. S. J.; Wrigglesworth, R.; Bevan, S. J.; Campbell, E. A.; Dray, A.; James, I. F.; Perkins, M. N.; Reid, D. J.; Winter, J. Analogues of Capsaicin with Agonist Activity as Novel Analgesic Agents: Structure-activity Studies: Part 1. The Aromatic 'A-Region'. *J. Med. Chem.* **1993**, *36*, 2362–2372.
(9) Walpole, C. S. J.; Wrigglesworth, R.; Bevan, S. J.; Campbell, E. A.; Dray, A.; James, I. F.; Perkins, M. N.; Masdin, K.; Winter, J. Analogues of Capsaicin with Agonist Activity as Novel Analgesic Agents: Structure-activity Studies: Part 2. The Amide-bond 'B-Region'. *J. Med. Chem.* **1993**, *36*, 2373–2380.
(10) Walpole, C. S. J.; Wrigglesworth, R.; Bevan, S. J.; Campbell, E. A.; Dray, A.; James, I. F.; Perkins, M. N.; Masdin, K. J.; Winter, J.

Analogues of Capsaicin with Agonist Activity as Novel Analgesic Agents: Structure-activity Studies: Part 3. The Hydrophobic Side-chain 'C-Region'. *J. Med. Chem.* **1993**, *36*, 2381–2389.
(11) Reviewed in Bevan, S.; Szolcsanyi, J. Sensory Neuron-specific Actions of Capsaicin: Mechanisms and Applications. *Trends Pharmacol. Sci.* **1990**, *11*, 330–333.
(12) Bevan, S.; Hothi, S.; Hughes, G.; James, I. F.; Rang, H. P.; Shah, K.; Walpole, C. S. J.; Yeats, J. C. Capsazepine: A Competitive Antagonist of the Sensory Neurone Excitant Capsaicin. *Br. J. Pharmacol.* **1992**, *107*, 544–552.
(13) Maggi, C. A.; Bevan, S. J.; Walpole, C. S. J.; Rang, H.; Giuliani, A. A Comparison of Capsazepine and Ruthenium Red as Capsaicin Antagonists in the Rat Urinary Bladder and Vas Deferens. *Br. J. Pharmacol.* **1993**, *108*, 801–805.
(14) Szallasi, A. *Neuropeptides* **1993**, *24* (4), 186, and personal communication.
(15) Liu, L.; Simon, S. A. A Rapid Capsaicin-Activated Current in Rat Trigeminal Ganglion Neurones. *Proc. Natl. Acad. Sci. U.S.A.* **1994**, *91*, 738–741.
(16) S. Bevan, personal communication.
(17) Buckwalter, B. L.; Lahann, T. R. Novel Urea Derivatives. Eur. Pat. Appl EP 0068590, 1982.
(18) Ushujima, R.; Nakagawa, S.; Elishi, M. Isoindoline Derivatives and Processes for their Preparation. Eur. Pat. Appl. EP 0227986 A1, 1987.
(19) Walpole, C. S. J.; Wrigglesworth, R., *et al.* Manuscript in preparation.
(20) See, for example: Masden, L. B.; Brehm, L.; Schaumberg, K.; Jorgensen, F. S.; Krogsgaard-Larsen, P. Relationship Between Structure, Conformational Flexibility, and Biological Activity of Agonists and Antagonists at the N-Methyl-D-Aspartic Acid Subtype of Excitatory Amino Acid Receptors. *J. Med. Chem.* **1990**, *33*, 374–380.
(21) Still, W. C.; Kahn, M.; Mitra, A. Rapid Chromatographic Technique for Preparative Separations with Moderate Resolution. *J. Org. Chem.* **1978**, *43*, 2923–2925.
(22) Perrin, D. D.; Armarego, W. L. F.; Perrin, D. R. *Purification of laboratory Chemicals*; Pergamon Press: New York, 1980.
(23) Kessler, H.; Griesinger, C.; Kerssebaum, R.; Wagner, K.; Ernst, R. R. Separation of Cross-relaxation and J Cross-peaks in 2D Rotating-frame. *J. Am. Chem. Soc.* **1987**, *109* (2), 607–609.
(24) Griesinger, C.; Ernst, R. R. Frequency Offset Effects and their Elimination in NMR Rotating-frame Cross-relaxation Spectroscopy. *J. Magn. Res.* **1987**, *75* (2), 261–271.
(25) Clark, M.; Cramer, R. D., III; van Opdenbosch, N. Validation of the General Purpose Tripos 5.2 Force Field. *J. Comput. Chem.* **1988**, *10* (8), 982–1021.
(26) Biosym Technologies Inc., San Diego, CA.
(27) Sandoz Pharma, Preclinical Department, unpublished results.
(28) Masdin, K. J.; Walpole, C. S. J.; Wrigglesworth, R. Preparation of N,N'-Dibenzyl and N-Benzyl, N'-phenethylthioureas as Analgesics and Antiinflammatories. U.K. Pat. Appl GB 2 206347 A, 1989.
(29) Cussans, N. J. Preparation of Tetrahydroquinolines as Anti-arrhythmic Agents. U.S. Pat. Appl US 4882337 A, 1989.